

EVALUATION OF INTERLAMINAR FRACTURE TOUGHNESS OF GLASS FIBER – EPOXY-MODIFIED COMPOSITE MATERIALS

SIVAKUMAR. C¹ & GEETHA SELVARANI. A²

¹Assistant Professor, Department of Mechanical Engineering, Vel Tech Rangarajan Dr. Sangunthala R & D
Institute of Science and Technology, Avadi, Chennai, Tamil Nadu, India

²Professor, Department of Civil Engineering, Vel Tech Rangarajan Dr. Sangunthala R & D
Institute of Science and Technology, Avadi, Chennai, Tamil Nadu, India

ABSTRACT

Developing efficient wind mill blades with high toughness and good fatigue life is one of the main engineering challenges for wind energy sector globally. FRP is commonly used in aerospace, manufacturing of auto ancillary parts, marine, and construction industries. Large wind mill blades are made of glass fiber/epoxy composites to achieve high-specific stiffness, strength and good fracture toughness. While operating, the wind mill blades are subjected to significant stress. These composite blades fail due to fiber/matrix delamination and cracking. Significant technical advances can be achieved by adding nano clay with glass fiber/epoxy composite. Toughness test (mode I) to understand the interlaminar fracture conducted on the double cantilever beam (DCB) specimen reveals that the inclusion of nano clay can appreciably increase the fracture toughness of the glass fiber/epoxy composite.

KEYWORDS: Glass Fiber, Nano Clay, Epoxy & Mode I

Received: Nov 01, 2017; **Accepted:** Nov 21, 2017; **Published:** Jan 08, 2018; **Paper Id.:** IJMPERDFEB201845

INTRODUCTION

Glass fiber-reinforced composite materials are known for their advanced engineering materials displaying high strength and low weight and its application in the automobile sectors, aerospace military, and sporting goods. Formed by reaction of an epoxide "resin" with polyamine "hardener," epoxy is a thermosetting polymer. Its applications are of wide range, including fiber-reinforced plastic materials and general purpose adhesives. The recent addition of nanoclay as an additive results in various desired effects that are currently used to modify the polymer performance. One of the most common nanoclays is montmorillonite, a very soft phyllosilicate mineral typically formed as microscopic crystals used in material applications. It consists of 1 nm thick aluminosilicate layers surface-substituted with metal cations and 10 µm-sized multilayer stacks. The surface modification of the clay layers can cause montmorillonite to disperse in a polymer matrix to form polymer-clay nanocomposite

According to previous studies, nanoclay and epoxy resin improved the fracture toughness, strength, and stiffness of the composites.

Carbon nanotubes are known to improve the mechanical properties of polymers but are not being widely used because of its high material cost. Nanoclay might increase the fracture toughness of epoxy and clay concentration when mixed with DGEBA epoxy resin using a mechanical stirrer. According to Antonio et al. [18],

the damping coefficient and the energy dissipation characteristic of the glass/epoxy composite using nanoclay particles improved. Hosur et al.[19] demonstrated improved impact characteristic of the composite sandwich structure using the nanoclay infused foam.

This study investigated the toughening effect of nanoclay mixed with epoxy. The composites are not isotropic materials and are anisotropic materials, showing different properties in various directions. Assessing the composites' outstanding properties can be achieved only if the loading direction coincides with the reinforcement direction. In many cases, the loading is multidirectional. Therefore, leading to various failures including delamination, matrix cracking and other type of fracture. The interlaminar fracture in the form of delamination is a major one that is commonly encountered. The delamination or interlaminar cracking is one of the principal modes of damage of composite structures. The intensification of delamination results in stiffness humiliation and ultimate failure of the composite structure. Different types of loading can lead to delamination. Resistance to delamination is also known as interlaminar fracture toughness. Thus, it is important to characterize the fracture behavior which enables the design of fiber-reinforced composite materials.

Double cantilever beam (DCB) test was used to measure fracture toughness with respect to the particle content at room temperature (25°C). The DCB is the most widely used test configuration for measuring mode I interlaminar fracture toughness. Using DCB specimens, extensive research has been conducted to study the influence of such factors as specimen dimensions, temperature, moisture, and loading rate on the mode I delamination behavior. In order to investigate their toughening mechanism, the fracture surface was also observed with SEM.

MATERIALS

In this study, the epoxy resin DGEBA used as matrix polymer and its very low viscosity and withstanding temperature at 25 °C is suited for resin infusion techniques. Apart from this, an epoxy hardener named Araldite HY 951 has been used. For each investigated nanoclay content, the fraction of this component is based on the manufacturer suggested neat epoxy (5:1). Modification of epoxy was achieved by commercial nanoclay, namely, I30P from Southern Clay Products (USA), which are surface-modified lamellae of montmorillonite with 1 nm thick and lateral dimensions ranging from 70 to 150 nm used as reinforcement for neat and epoxy-modified laminates. Fiber materials can be used as e-glass fibers.

Epoxy Modification and Laminate Fabrication using Epoxy + Hardner of 100:10 Ratio

Table 1: Nano Clay

S. NO	Grade	Sample %				
1	I30P	2	4	6	8	10

Table 2: Mixture Calculation(in gms)

S. No	Percentage	Nanoclay	Hardner	Epoxy
1	2	4.0	19.6	176.4
2	4	8.0	19.2	172.8
3	6	12.0	18.8	169.2
4	8	16.0	18.4	165.6
5	10	20.0	18.0	162.0

Initially epoxy was measured volumetrically, taking 1000 ml double-neck flask and continuously heating upto 50°C and stirring it using mechanical stirrer and maintaining the temperature upto 65°C. In the mean time, nanoclay was

dissolved in solvent acetone and stirred well by glass rod as shown in tables 1& 2. This mixture was poured into epoxy resin and the stirring continued for 1 hr at temperature of 65°C.

After reaching finer results, the mixture was sonicated. The sonication process is shown in figure 1 and is always operated with the maximum power amplitude of 200 W, and various duty cycles (25%, 50%, and 75%) were chosen, in order to investigate its effect on the fracture toughness. The process was continued for 40 min followed by molding preceding an extensive degassing process, thereby reducing the amount of trapped air and avoiding voids in the matrix using low-vacuum pump.



Figure 1: Sonicator

After 30 min, most air was released to form a brownish mixture of modified resin [AQ: Please check whether the edit retains the intended sense of the sentence.]. At the end of the degassing process, the modified resin should be devoid of any bubble and translucent materials as shown in figure. 2. CT specimens were manufactured by simply pouring the resin into a silicone mold. The dimensions of the specimens were in agreement with the specifications suggested by ASTM.

Laminates were fabricated using compressor molding. Mold was cleaned by acetone and wax applied to the mold surface. Before processing, the fibers are sized into 27 cm × 27cm. First, the resin was applied to the mould, placed on the fiber, and continued the process upto 14 layers, that is, where 14 layers of twill glass fabric were stacked up. The resulting laminate thickness was about 3 mm. All the fabric layers were placed based on their warp direction parallel to the longitudinal direction of the mold. A Teflon film of 50 µm thick was used to create a pre-crack on the DCB specimens. Teflon film was placed after the seventh layer in the stack following which the pressure was applied and the temperature maintained upto 80°C for 2 hr. Geometry and size of specimens were those suggested by ASTM D 5528-01. De molding performed after complete curing at room temperature.

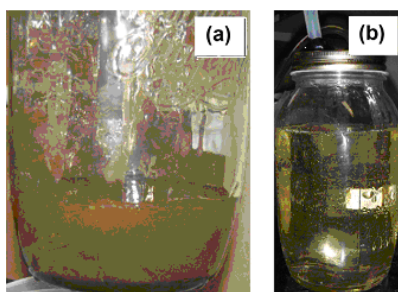


Figure 2: Nano Modified Resin Appearance:

(a) After 30 min Degassing and (b) At the End of Degassing Process

Interlaminar (Delamination) Fracture Toughness

Interlaminar fracture is one of the most important problems for FRP composites and it reduces the stiffness of the components. Delamination failure influences the performance of laminated composites where geometrical and material discontinuities exist. Delamination and its growth are characterized by strain energy release rate (G) and the manner in which the load was applied. A delamination may be loaded in Mode I (tensile), Mode II (shear), Mode III (tearing shear), or it may be loaded in a combination of these modes. Depending on the mode of loading, the delamination actually begins to extend significantly, indicating is the critical strain energy release rate (G_c).

Delamination resistance may be characterized based on various test methods. ASTM is working on standards to measure G_{Ic} under a variety of loading conditions. ASTM D5528 recommends DCB test to measure the Mode I fracture toughness G_{Ic} [AQ: Please check whether it is G_{Ic} or G_{Ic} as both forms are used in the article.] of fiber-reinforced polymer composites. The end notch flexure (ENF) test measures the pure Mode II fracture toughness G_{IIc} .

RESULTS AND DISCUSSIONS

Mode I Interlaminar Fracture Toughness Testing

DCB is the preferred specimen type in most Mode I interlaminar fracture test, consisting of a rectangular uniform thickness unidirectional laminated composite specimen as shown schematically in Figure

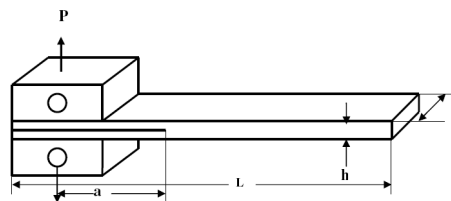


Figure 3: Double Cantilever Beam Specimen with Load Blocks used for Mode I Testing

In the mid plane of the laminate, a non adhesive Teflon film was inserted during fabrication, in turn acting as a delamination initiator. On the top and bottom surfaces of the DCB specimen arms the loading blocks were mounted. With a constant cross-head speed of 1-5 mm/min, the delaminated end of the DCB specimen was opened by quasi-static loading at a displacement control mode. During the test, delamination lengths are determined visually. For more accurate delamination length readings, ASTM recommends using a travelling microscope.

Interlaminar Fracture Toughness: G_{Ic} Calculations

The interlaminar fracture toughness calculation is based on beam theory (with corrections for load blocks), experimental compliance calibration, or a modified compliance calibration, as described by ASTM D5528 [20]. Three methods were used to calculate G_{Ic} values, which differed by not more than 3.1 %, and none of the method was superior to the others. Since it yielded the most repeated G_{Ic} values for 80% of specimens tested, modified beam theory (MBT) method is recommended.

Modified Beam Theory (MBT) Method [AQ: Please Fix the Equations in Math type]

$$G_I = \frac{3P\delta}{2b a}$$

P = load,

δ = load point displacement,

b = specimen width

a = delamination length

Compliance Calibration (CC) Method

$$G_I = \frac{nP\delta}{2b a}$$

Modified Compliance Calibration (MCC) Method

$$G_I = \frac{3P^2 C^{2/3}}{2S_1 b h}$$

After testing, the values are applied to modified beam theory to calculate the G1c as shown in tables 3 to 8.

Table 3: Neat Epoxy [AQ: Please Fix the Tables 3 to 8 in Editable Format]

a	Pc	d	c	c 1/3	logc	loga	a/h	dC/da	G1cCBT
50	110.2	10.7	0.097096	1	-1.0128	1.69897	16.66667	0.022437	1.414968
51	7.9	11.8	1.493671	1.142949	0.174255	1.70757	17	0.0236	0.109671
52	40.5	13	0.320988	0.684953	-0.49351	1.716003	17.33333	0.024799	0.6075
53	20.8	13.3	0.639423	0.861643	-0.19421	1.724276	17.66667	0.026033	0.313177
54	12.3	14.6	1.186992	1.058744	0.074448	1.732394	18	0.027305	0.199533
55	16.2	15.6	0.962963	0.987511	-0.01639	1.740363	18.33333	0.028614	0.275695
60	45.4	17.6	0.387685	0.729384	-0.41154	1.778151	20	0.035726	0.79904
65	56.8	20.3	0.357394	0.709902	-0.44685	1.812913	21.66667	0.04382	1.064345
70	46.8	22.9	0.489316	0.788194	-0.31041	1.845098	23.33333	0.05294	0.918617
75	40.7	27.1	0.665848	0.873341	-0.17663	1.875061	25	0.063129	0.882376
80	40.2	31.7	0.788557	0.923944	-0.10317	1.90309	26.66667	0.074429	0.955755
85	36.2	35.4	0.977901	0.992586	-0.00971	1.929419	28.33333	0.086879	0.904574
90	34.8	40.9	1.175287	1.055256	0.070144	1.954243	30	0.100519	0.94888
95	40.7	45.9	1.127764	1.040851	0.052218	1.977724	31.66667	0.115386	1.179872
96	32.2	47.6	1.478261	1.139009	0.169751	1.982271	32	0.11851	0.95795
97	31.1	47.8	1.536977	1.153879	0.186668	1.986772	32.33333	0.121685	0.919534
98	35.2	48.1	1.366477	1.109572	0.135602	1.991226	32.66667	0.124912	1.036604
99	35.3	48.6	1.376771	1.112349	0.138862	1.995635	33	0.128189	1.039745
100	36.4	49.3	1.354396	1.106296	0.131746	2	33.33333	0.131519	1.076712
									0.78831

Table 4: Two Percent Laminate

a	Pc	d	c	c 1/3	logc	loga	a/h	dC/da	G1cCBT
50	125.5	10.7	0.085259	1	-1.06926	1.69897	16.66667	0.022437	1.61142
51	20.3	11.8	0.581281	0.834719	-0.23661	1.70757	17	0.0236	0.281812
52	55.3	13	0.235081	0.61747	-0.62878	1.716003	17.33333	0.024799	0.8295
53	35.9	13.3	0.370474	0.718449	-0.43124	1.724276	17.66667	0.026033	0.540532
54	25.9	14.6	0.563707	0.826229	-0.24895	1.732394	18	0.027305	0.420156
55	34.8	15.6	0.448276	0.765534	-0.34845	1.740363	18.33333	0.028614	0.592233
60	66.2	17.6	0.265861	0.643295	-0.57535	1.778151	20	0.035726	1.16512
65	72.2	20.3	0.281163	0.655395	-0.55104	1.812913	21.66667	0.04382	1.352917
70	63.2	22.9	0.362342	0.713159	-0.44088	1.845098	23.33333	0.05294	1.240526
75	54.9	27.1	0.493625	0.790499	-0.3066	1.875061	25	0.063129	1.190232
80	51.9	31.7	0.61079	0.848598	-0.21411	1.90309	26.66667	0.074429	1.233923
85	53.9	35.4	0.656772	0.869359	-0.18259	1.929419	28.33333	0.086879	1.346866
90	54.8	40.9	0.74635	0.907173	-0.12706	1.954243	30	0.100519	1.494213
95	52.8	45.9	0.869318	0.954435	-0.06082	1.977724	31.66667	0.115386	1.530644
96	51.2	47.6	0.929688	0.976014	-0.03166	1.982271	32	0.11851	1.5232
97	56	47.8	0.853571	0.948643	-0.06876	1.986772	32.33333	0.121685	1.655753
98	57	48.1	0.84386	0.945035	-0.07373	1.991226	32.66667	0.124912	1.678592
99	58	48.6	0.837931	0.942819	-0.07679	1.995635	33	0.128189	1.708364
100	60	49.3	0.821667	0.936685	-0.0853	2	33.33333	0.131519	1.7748
									1.197743

Table 5: Four Percent Laminate

a	Pc	d	c	c 1/3	logc	loga	a/h	dC/da	G1cCBT
50	123	10.7	0.086992	1	-1.06052	1.69897	16.66667	0.022437	1.57932
51	17.2	11.8	0.686047	0.882075	-0.16365	1.70757	17	0.0236	0.238776
52	52.3	13	0.248566	0.629046	-0.60456	1.716003	17.33333	0.024799	0.7845
53	34.5	13.3	0.385507	0.728029	-0.41397	1.724276	17.66667	0.026033	0.519453
54	24.8	14.6	0.58871	0.838257	-0.2301	1.732394	18	0.027305	0.402311
55	32.5	15.6	0.48	0.783165	-0.31876	1.740363	18.33333	0.028614	0.553091
60	62.3	17.6	0.282504	0.656434	-0.54898	1.778151	20	0.035726	1.09648
65	71.5	20.3	0.283916	0.657525	-0.54681	1.812913	21.66667	0.04382	1.3398
70	62.5	22.9	0.3664	0.715809	-0.43604	1.845098	23.33333	0.05294	1.226786
75	53.5	27.1	0.506542	0.797328	-0.29538	1.875061	25	0.063129	1.15988
80	48.9	31.7	0.648262	0.865591	-0.18825	1.90309	26.66667	0.074429	1.162598
85	50.9	35.4	0.695481	0.886097	-0.15771	1.929419	28.33333	0.086879	1.271901
90	51.9	40.9	0.788054	0.923747	-0.10344	1.954243	30	0.100519	1.41514
95	48.9	45.9	0.93865	0.979138	-0.0275	1.977724	31.66667	0.115386	1.417585
96	47	47.6	1.012766	1.004233	0.005609	1.982271	32	0.11851	1.39825
97	51.5	47.8	0.928155	0.975478	-0.03238	1.986772	32.33333	0.121885	1.522701
98	54	48.1	0.890741	0.962204	-0.05025	1.991226	32.66667	0.124912	1.590245
99	53.5	48.6	0.908411	0.968519	-0.04172	1.995635	33	0.128189	1.575818
100	54	49.3	0.912963	0.970132	-0.03955		2	0.131519	1.59732
									1.126258

Table 6: Six Percent Laminate

a	Pc	δ	c	c 1/3	logc	loga	a/h	dC/da	G1c(MBT)
50	117.33	10.7	0.091196	1	-1.04003	1.69897	16.66667	0.022437	1.506517
51	13.28	11.8	0.888554	0.961417	-0.05132	1.70757	17	0.0236	0.184358
52	47.54	13	0.273454	0.649355	-0.56312	1.716003	17.33333	0.024799	0.7131
53	28.82	13.3	0.461485	0.772973	-0.33584	1.724276	17.66667	0.026033	0.433931
54	20.34	14.6	0.717797	0.895465	-0.144	1.732394	18	0.027305	0.32996
55	26.01	15.6	0.599769	0.843468	-0.22202	1.740363	18.33333	0.028614	0.442643
60	57.44	17.6	0.306407	0.674431	-0.5137	1.778151	20	0.035726	1.010944
65	66.8	20.3	0.303892	0.672583	-0.51728	1.812913	21.66667	0.04382	1.251729
70	56.89	22.9	0.402531	0.738581	-0.3952	1.845098	23.33333	0.05294	1.116669
75	48.07	27.1	0.563761	0.826256	-0.2489	1.875061	25	0.063129	1.042158
80	50.19	31.7	0.6316	0.858118	-0.19956	1.90309	26.66667	0.074429	1.193267
85	44.26	35.4	0.799819	0.928317	-0.09701	1.929419	28.33333	0.086879	1.105979
90	46.8	40.9	0.873932	0.956119	-0.05852	1.954243	30	0.100519	1.27608
95	48.78	45.9	0.940959	0.979939	-0.02643	1.977724	31.66667	0.115386	1.414107
96	44.21	47.6	1.076679	1.024908	0.032086	1.982271	32	0.11851	1.315248
97	43.12	47.8	1.108534	1.034907	0.044749	1.986772	32.33333	0.121885	1.274929
98	47.22	48.1	1.018636	1.006168	0.008019	1.991226	32.66667	0.124912	1.390581
99	46.38	48.6	1.047865	1.015691	0.020306	1.995635	33	0.128189	1.366102
100	48.49	49.3	1.016704	1.005532	0.007195		2	0.131519	1.434334
									1.016451

Table 7: Eight Percent Laminate

a	Pc	δ	c	c 1/3	logc	loga	a/h	dC/da	G1c(MBT)
50	121.77	10.7	0.087871	1	-1.05616	1.69897	16.66667	0.022437	1.563527
51	15.65	11.8	0.753994	0.910256	-0.12263	1.70757	17	0.0236	0.217259
52	49.99	13	0.260052	0.63858	-0.58494	1.716003	17.33333	0.024799	0.74985
53	31.33	13.3	0.424513	0.751775	-0.37211	1.724276	17.66667	0.026033	0.471723
54	22.55	14.6	0.64745	0.86523	-0.18879	1.732394	18	0.027305	0.365811
55	29.66	15.6	0.525961	0.807379	-0.27905	1.740363	18.33333	0.028614	0.504759
60	60	17.6	0.293333	0.664709	-0.53264	1.778151	20	0.035726	1.056
65	68.77	20.3	0.295187	0.666104	-0.5299	1.812913	21.66667	0.04382	1.288644
70	58.99	22.9	0.388201	0.72972	-0.41094	1.845098	23.33333	0.05294	1.157889
75	51.02	27.1	0.531164	0.81003	-0.27477	1.875061	25	0.063129	1.106114
80	46.95	31.7	0.675186	0.877401	-0.17058	1.90309	26.66667	0.074429	1.116236
85	48.9	35.4	0.723926	0.898004	-0.14031	1.929419	28.33333	0.086879	1.221925
90	50.05	40.9	0.817183	0.93498	-0.08768	1.954243	30	0.100519	1.364697
95	46.95	45.9	0.977636	0.992496	-0.00982	1.977724	31.66667	0.115386	1.361056
96	45.55	47.6	1.045005	1.014767	0.019119	1.982271	32	0.11851	1.355113
97	49.2	47.8	0.971545	0.990433	-0.01254	1.986772	32.33333	0.121885	1.454697
98	52	48.1	0.925	0.974373	-0.03386	1.991226	32.66667	0.124912	1.531347
99	51	48.6	0.952941	0.984077	-0.02093	1.995635	33	0.128189	1.502182
100	53	49.3	0.930189	0.97619	-0.03143		2	0.131519	1.56774
									1.077391

Table 8: Ten Percent Laminate

a	Pc	δ	c	c 1/3	logc	loga	a/h	dC/da	G1c(MBT)
50	123.88	10.7	0.086374	1	-1.06362	1.69897	16.66667	0.022437	1.590619
51	17.99	11.8	0.65592	0.868983	-0.18315	1.70757	17	0.0236	0.249744
52	51.85	13	0.250723	0.630858	-0.60081	1.716003	17.33333	0.024799	0.77775
53	33.33	13.3	0.39904	0.736442	-0.39898	1.724276	17.66667	0.026033	0.501837
54	24.55	14.6	0.594705	0.84109	-0.2257	1.732394	18	0.027305	0.398256
55	31.77	15.6	0.491029	0.789112	-0.30889	1.740363	18.33333	0.028614	0.540668
60	62	17.6	0.283871	0.65749	-0.54688	1.778151	20	0.035726	1.0912
65	70.65	20.3	0.287332	0.660149	-0.54162	1.812913	21.66667	0.04382	1.323872
70	61.2	22.9	0.374183	0.720837	-0.42692	1.845098	23.33333	0.05294	1.201269
75	52.55	27.1	0.515699	0.802099	-0.2876	1.875061	25	0.063129	1.139284
80	49	31.7	0.646939	0.865003	-0.18914	1.90309	26.66667	0.074429	1.164975
85	51.99	35.4	0.6809	0.879867	-0.16692	1.929419	28.33333	0.086879	1.299138
90	52.55	40.9	0.778306	0.919927	-0.10885	1.954243	30	0.100519	1.432863
95	49.99	45.9	0.918184	0.971976	-0.03707	1.977724	31.66667	0.115386	1.449184
96	47.85	47.6	0.994775	0.998257	-0.00227	1.982271	32	0.11851	1.423538
97	51.65	47.8	0.92546	0.974534	-0.03364	1.986772	32.33333	0.121685	1.527136
98	54	48.1	0.890741	0.962204	-0.05025	1.991226	32.66667	0.124912	1.590245
99	53.77	48.6	0.90385	0.966897	-0.0439	1.995635	33	0.128189	1.583771
100	55	49.3	0.896364	0.964222	-0.04752		2	33.33333	0.131519
									1.6269
									1.128979

Table 9: Result and Summary

Composite Laminates	Mode 1
	G1c(MBT)
Neat epoxy	0.78031
2%	1.197743
4%	1.126258
6%	1.016451
8%	1.077391
10%	1.128979

CONCLUSIONS

This study presents the preliminary experimental results of assessing the benefits derived from the matrix nano modification of composite laminates made by compression molding on glass fabrics. The experimental program was aimed at investigating the following properties: mode I fracture toughness and crack propagation resistance for neat and clay-modified epoxy. The study results indicate significant improvements in the fracture toughness and crack propagation threshold of clay-modified epoxy.

REFERENCES

1. Lan T, Pinnavaia TJ. Clay-reinforced epoxy nanocomposites. *Chem Mater* 1994;6:2216–9.
2. Liu WP, Hoa SV, Pugh M. Organoclay-modified high performance epoxy nanocomposites. *Compos Sci Technol* 2005;65:307–16.
3. Messerlith PB, Giannelis EP. Synthesis and characterization of layered silicate–epoxy nanocomposites. *Chem Mater* 1994;6:1719–25.
4. Boo WJ, Liu, Sue HJ. Fracture behaviour of nanoplatelet reinforced polymer nanocomposites. *Mater Sci Tech* 2006;22:829–34.
5. Sue HJ, Gam KT, Bestaoui N, Clearfield A, Miyamoto M, Miyatake N. Fracture behavior of α -zirconium phosphate-based epoxy nanocomposite. *Acta Materialia* 2004;52:2239–50.
6. Zerda AS, Lesser AJ. Intercalated clay nanocomposites: Morphology, mechanics, and fracture behaviour. *J Polym Sci: Part B: Polym Phys* 2001;39:1137–46.

7. Kornmann X, Berglund LA, Sterte J. Nanocomposite based on montmorillonite and unsaturated polyester. *Polym Eng Sci* 1998;38:1351–8.
8. Zilg C, Mulhaupt R, Finter J. Morphology and toughness/stiffness balance of nanocomposites based upon anhydride-cured epoxy resins and layered silicates. *Macromol Chem Phys* 1999;200:661–70.
9. Sandler J, Shaffer MSP, Prasse T, Bauhofer W, Schulte K, Windle AH. Development of a dispersion process for carbon nanotubes in an epoxy matrix and the resulting electrical properties. *Polymer* 1999;40:5967–71.
10. Martin CA, Sandler JKW, Shaffer MSP, Schwarz MK, Bauhofer W, Schulte K, et al. Formation of percolating networks in multi-wall carbon nanotube-epoxy composites. *Compos Sci Technol* 2004;64:2309–16.
11. Gojny FH, Wichmann MHG, Köpke U, Fiedler B, Schulte K. Carbon nanotubereinforced epoxy-composites: enhanced stiffness and fracture toughness at low nanotube content. *Compos Sci Technol* 2004;64:2363–71.
12. Florian HG, Malte HG, Bodo F, Karl S. Influence of different carbon nanotubes on the mechanical properties of epoxy matrix composites – a comparative study. *Compos Sci Technol* 2005;65:2300–13.
13. Usuki A, Kojima Y, Kawasumi M, Okada A, Fukushima Y, Kurauchi T, et al. Synthesis of nylon 6-clay hybrid. *J Mater Res* 1993;8:1179.
14. Weiping L, Suong VH, Martin P. Fracture toughness and water uptake of highperformance epoxy/nanoclay nanocomposites. *Compos Sci Technol* 2005;65:2364–73.
15. Lei W, Ke W, Ling C, Yongwei Z, Chaobin H. Preparation, morphology and thermal/mechanical properties of epoxy/nanoclay composite. *Compos Part A* 2006;37:1890–6.
16. Qi B, Zhang QX, Bannister M, Mai YW. Investigation of the mechanical properties of DGEBA-based epoxy resin with nanoclay additives. *Compo Struct* 2006;75:514–9.
17. Ho MW, Lam CK, Lau KT, Dickon HL, David H. Mechanical properties of epoxybased composites using nanoclays. *Compos Struct* 2006;75:415–21.
18. ALLIX O., LEVEQUE D., PERRET L. Identification and forecast of delamination in composite laminates by an interlaminar interface model. *Composites Science and Technology* 1998;58:671–678
19. BAZHENOV S. L. Longitudinal splitting in unidirectional fibre-reinforced composites with can open hole. *Composites Science and Technology* 1998;58:83–89
20. [20] M. S. Sham Prasad*1, C. S. Venkatesha2, T. Jayaraju, 'Experimental Methods of Determining Fracture Toughness of Fiber Reinforced Polymer Composites under Various Loading Conditions,' *Journal of Minerals & Materials Characterization & Engineering*, Vol. 10, No.13, pp.1263-1275, 2011
21. Sabita Rani Sahoo, A. Mishra''Fracture Characterization of Plain Woven''Fabric Glass-Epoxy Composites *World Academy of Science, Engineering and Technology* 67 2012
22. Fracture and interlaminar properties of clay-modified epoxies ""and their glass reinforced laminates
23. Marino Quaresimin ↑, Marco Salviato, Michele Zappalorto *Engineering Fracture Mechanics* 81 (2012) 80–93